Chapter 20
Normative Retinal Thicknesses in Common Animal Models of Eye Disease Using Spectral Domain Optical Coherence Tomography

Christy L. Carpenter, Alice Y. Kim, and Amir H. Kashani

Abstract

Purpose

This study demonstrates a standardized approach to measuring retinal thickness (RT) using spectral domain optical coherence tomography (SD-OCT) in commonly used animal models of disease and reports a normative data set for future use.

Materials and Methods

Twenty normal eyes of 4 adult animal models (5 rats, 5 rabbits, 5 canines, and 5 mini-pigs) were used. Manual measurements were made on the commercially available Heidelberg Spectralis™ SD-OCT to determine the total, inner, and outer retinal thickness (RT) at fixed distances from the optic nerve head (ONH) (1, 2, 3, 4, 5, and 6 mm away) in order to control for normal variation in retinal thickness. Analysis of variance (ANOVA) with P value <0.05 indicated statistical significance.

Results

Total RT significantly decreased with increasing distance from the ONH for the canine, mini-pig, and rabbit vascular models. Inner RT significantly decreased for the canine, mini-pig, rabbit vascular, and rabbit avascular models; and outer RT significantly decreased for only the canine model. Among the animal models, RT at similar distances from the ONH were significantly different for total, inner, and outer RT.

Conclusion

There are significant differences in the total, inner, and outer RT of normal canine, mini-pig, rabbit, and rat retinas with SD-OCT using a standardized approach.

C. L. Carpenter · A. Y. Kim
Department of Ophthalmology, USC Eye Institute, Keck School of Medicine of the University of Southern California, Los Angeles, California, USA

A. H. Kashani (✉)
Department of Ophthalmology, USC Eye Institute, Keck School of Medicine of the University of Southern California, Los Angeles, California, USA

USC Roski Eye Institute, Los Angeles, CA, USA
e-mail: ahkashan@usc.edu

These measurements provide a normative reference for future studies and illustrate a standardized method of assessing RT.

20.1 Introduction

Spectral domain optical coherence tomography (SD-OCT) is a noninvasive imaging modality that uses the unique light-scattering properties of biological tissue to capture the structural characteristics of the retina (Drexler and Fujimoto 2008). SD-OCT findings correlate very well with histological sections of the same animal model (Costa et al. 2006; Remtulla and Hallett 1985; Kim et al. 2008; Nagata et al. 2009). In addition, morphological dimensions such as RT can be measured with high reproducibility, as found in previous studies with humans and animal models (Costa et al. 2006; Remtulla and Hallett 1985; Kim et al. 2008; Nagata et al. 2009; Hernandez-Merino et al. 2011; Rosolen et al. 2012; Ferguson et al. 2013; Ruggeri et al. 2007; Alkin et al. 2013; Ducros et al. 1999; Gilger 2014; Srinivasan et al. 2006; Ferguson et al. 2014; Sadda et al. 2007; Garcia Garrido et al. 2014). However, comparisons of RT between various animal models as well as normative data for commonly used animal models using SD-OCT are lacking in the current literature. The purpose of this study is to establish a standardized protocol and normative data set for measuring total, inner, and outer RT for common animal models. Rats, rabbits, mini-pigs, and canines were chosen for this study based on their common use in studies on ophthalmic disease (Remtulla and Hallett 1985; Kim et al. 2008; Nagata et al. 2009; Hernandez-Merino et al. 2011; Rosolen et al. 2012; Ferguson et al. 2013; Ruggeri et al. 2007; Alkin et al. 2013; Ducros et al. 1999; Gilger 2014; Srinivasan et al. 2006). Using SD-OCT to quantify RT among multiple animal models is integral to the reliability and reproducibility of future studies using these animal models.

## 20.2 Materials and Methods

20.2.1 Experiments with Animals

The OCT database of the USC vivarium was reviewed for the records of animals that had undergone OCT imaging as part of previously approved protocols. Institutional Animal Care and Use Committee (IACUC) approved studies at USC only allow invasive procedures and studies of a single eyes. The contralateral eye is commonly used as a control. The OCT database was reviewed to identify OCT images from the control eye of such animals at baseline for this study. Therefore,

this was a retrospective, secondary analysis of OCT data from the control eyes of animals that were used for various studies of the retina under previously approved IACUC protocols. The health, safety, and comfort of all the animals were ensured under appropriate IACUC practices of the University of Southern California. Twenty eyes of 20 animals were identified as follows: 5 eyes of 5 pigmented Copenhagen rats, 5 eyes of 5 pigmented New Zealand rabbits, 5 eyes of 5 pigmented Göttingen mini-pigs, and 5 eyes of 5 pigmented beagle canines. All animals were imaged under standard imaging protocols and appropriate anesthesia. Pupils were dilated with phenylephrine hydrochloride 2.5% and tropicamide 0.5% eye drops.

20.2.2 Imaging Methods

A commercially available Spectralis™ HRA + OCT device (Heidelberg Engineering, Heidelberg, Germany) was used for imaging. A dense raster scan of 48 B-scans, each separated by 120 μm acquired over a field of 20 × 15 degrees (horizontal × vertical), was used in each animal. At least three raster scans for the specified areas of each eye were taken. Twenty SD-OCT images with good or excellent signal-to-noise ratio were selected for analysis. Images were assessed as "good" or "excellent" based on the readers ability to clearly distinguish a distinctive border between the vitreous humor and the inner limiting membrane (ILM), a distinctive border between the outer plexiform layer (OPL) and outer nuclear layer (ONL), and a distinctive border of the hyperreflective retinal pigment epithelium (RPE) band and interdigitation zone (IDZ).

Total RT was defined as the linear distance between the ILM and the RPE as measured by the manual caliper tool. The inner RT was defined as the distance between the ILM and the anterior edge of the ONL. The outer RT was defined as the distance between the anterior border of the ONL and the RPE. This segmentation scheme is depicted in Fig. 20.1. The total, inner, and outer RT were manu-
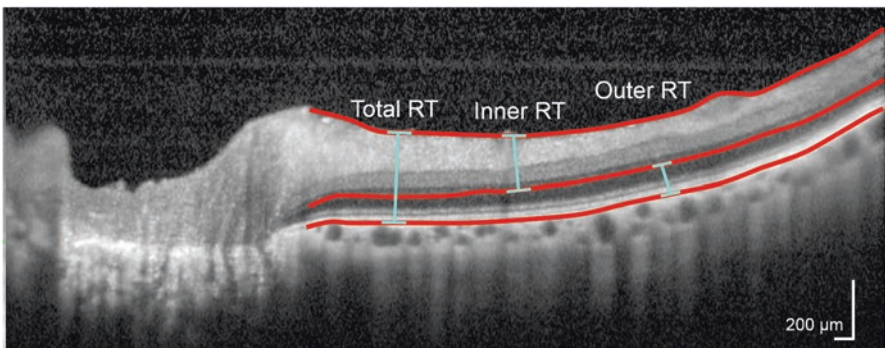
Fig. 20.1 Normal porcine retinal layer definitions. Red lines denote the boundaries between layers. Layer measurements used in this study include inner, outer, and total RT
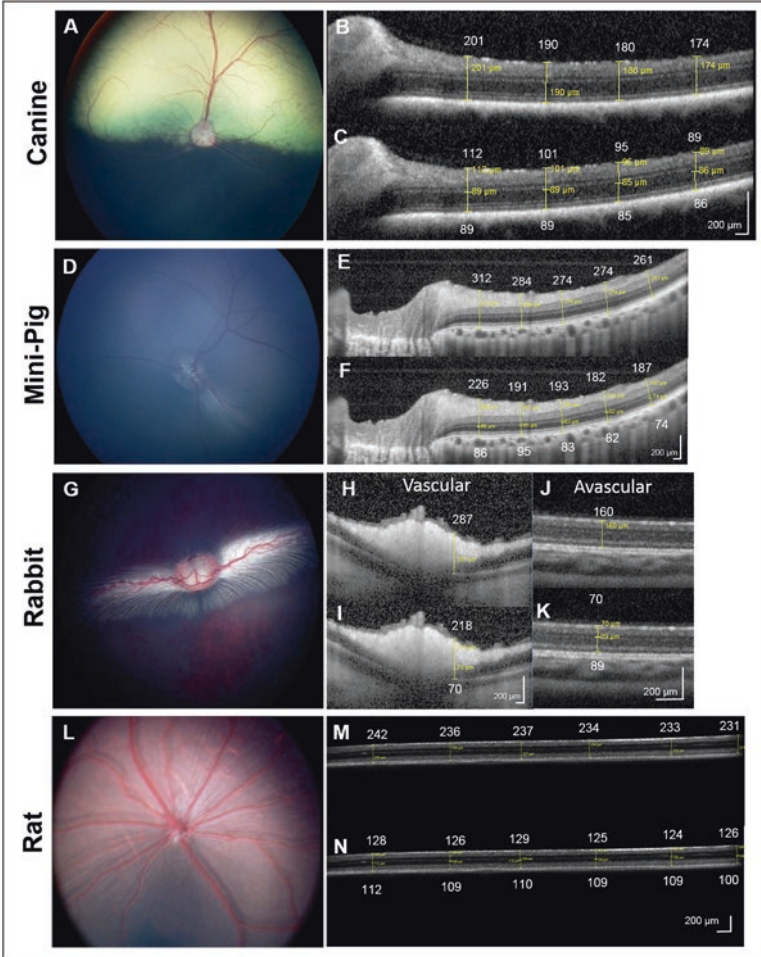
Fig. 20.2 Color fundus images and retinal thickness measurements of healthy (**a–c**) canine, (**d–f**) mini-pig, (**g–k**) rabbit, and (**l–n**) rat retinas. For each animal model, representative color fundus images are shown on the left and SD-OCT scans are to the right. The top SD-OCT scan shows the total RT, and the bottom SD-OCT scan shows the inner and outer RT. The rabbit retina was measured in two regions: the (**h**, **i**) vascular area and the (**j**, **k**) avascular area. Measurements are recorded in white along with the original caliper measures in yellow for clarity (all measurements in microns)

ally measured at 1, 2, 3, 4, 5, and 6 mm from the ONH. Distances from the ONH were measured as a line starting from the edge of the ONH and extending radially (Fig. 20.2).

20.2.3   Statistics

The mean and standard deviations of RT measurements were calculated at each distance from the ONH and recorded in microns (μm). RT values were compared at each distance from the ONH within each animal model and between the different animal models at each distance. Analysis of variance (ANOVA) values were calculated using Soper's analysis of variance calculator (Wiley, New York, NY) with $p < 0.05$ for significance.

20.3   Results

Table 20.1 shows the mean RT at 1, 2, 3, 4, 5, and 6 mm from the ONH as well as the results of ANOVA analysis. Table 20.2 shows the results of ANOVA analysis when comparing values among the animal models at each distance from the ONH. There were several instances in which the image of the peripheral retina was too unclear to measure the farthest distances. Among canines, there was poor visualization past the 3 mm or 4 mm mark in 4 subjects. Among mini-pigs, there was poor visualization past the 5 mm mark in 4 subjects. Among rabbits, there was poor visualization past the 4 mm or 5 mm mark in 4 subjects. Among rats, there was poor visualization past the 3 mm, 4 mm, or 5 mm mark in 3 subjects. In these cases, the RT measurements were not included in the subsequent analysis to maintain integrity of the analysis.

In the canine, the mean total RT decreased significantly with increasing distance from the ONH from 207 to 164 μm (Fig. 20.2a–c). The inner RT also decreased from 111.6 to 79 μm, and the outer RT decreased from 95.4 to 86 μm ($p < 0.001$ for all). This animal model showed the only statistically significant difference found for outer RT ($p = 0.016$).

In the mini-pig animal model (Fig. 20.2d–f), there was a relatively steady decrease in mean total RT. Both the total and inner RT decreased significantly from 327 to 245 μm and 221 to 149 μm, respectively ($p < 0.001$ for both). The outer RT decreased from 105 to 96 μm but was not statistically significant ($p = 0.559$).

In the rabbit model (Fig. 20.2g–k), the mean RT for the vascular area of the retina decreased most dramatically compared to all of the animal models observed. The total vascular RT decreased significantly from 341 to 163 μm, and the vascular inner RT decreased from 252 to 121 μm at increasing distance from the ONH ($p < 0.001$ for all). However, there were no statistically significant differences in the outer RT of the vascular section of the eye ($p = 0.456$). For the avascular regions of the rabbit eyes, only the mean inner RT showed statistically significant changes as it decreased from 75 to 55 μm ($p < 0.001$). The avascular total RT, which decreased from 168 to 142 μm, and the avascular outer RT, which decreased from 98 to 87 μm, were not statistically different ($p = 0.069$ and 0.402, respectively).

**Table 20.1** Total, inner, and outer retinal thicknesses for each animal model

Distance from ONH (mm)	1	2	3	4	5	6	P value
Mean total RT (µm)							Total RT
Canine	207.00 ± 7.58	198.00 ± 7.97	191.00 ± 6.16	184.00 ± 11.02	178.00 ± 0.00	164.00 ± 0.00	<0.001*
Mini-pig	327.40 ± 10.21	311.60 ± 15.01	293.80 ± 11.50	281.00 ± 16.55	264.60 ± 13.81	245.00 ± 0.00	<0.001*
Rabbit V	340.80 ± 5.17	294.80 ± 9.73	246.60 ± 9.21	214.80 ± 20.29	189.00 ± 19.70	163.00 ± 0.00	<0.001*
Rabbit AV	168.40 ± 13.30	162.80 ± 14.29	162.00 ± 16.55	156.60 ± 18.40	153.50 ± 14.01	142.00 ± 0.00	0.07
Rat	235.80 ± 16.63	230.40 ± 18.39	226.00 ± 18.95	223.75 ± 20.43	229.00 ± 17.35	219.50 ± 0.00	0.73
Mean inner RT (µm)							Inner RT
Canine	111.60 ± 5.94	105.00 ± 4.64	99.80 ± 4.15	94.30 ± 6.11	89.00 ± 0.00	79.00 ± 0.00	<0.001*
Mini-pig	221.60 ± 8.11	208.40 ± 10.88	193.00 ± 8.09	183.20 ± 9.98	168.80 ± 11.39	149.00 ± 0.00	<0.001*
Rabbit V	252.25 ± 14.31	207.50 ± 12.56	168.00 ± 19.58	144.25 ± 28.36	121.00 ± 39.60	–	<0.001*
Rabbit AV	75.00 ± 8.25	70.00 ± 7.48	68.50 ± 5.00	65.25 ± 4.27	58.25 ± 3.30	55.00 ± 0.00	<0.001*
Rat	125.40 ± 6.69	122.60 ± 9.73	119.80 ± 10.11	118.75 ± 11.18	120.00 ± 8.72	118.50 ± 0.00	0.77
Mean outer RT (µm)							Outer RT
Canine	95.40 ± 4.77	93.00 ± 4.24	89.60 ± 5.08	90.33 ± 5.03	89.00 ± 0.00	86.00 ± 0.00	0.016*
Mini-pig	105.80 ± 12.95	103.20 ± 12.64	100.80 ± 11.08	97.80 ± 9.88	95.80 ± 8.53	96.00 ± 0.00	0.56
Rabbit V	89.00 ± 9.13	84.00 ± 10.55	79.75 ± 10.97	75.25 ± 12.82	76.00 ± 19.80	–	0.46
Rabbit AV	97.75 ± 11.87	97.75 ± 9.71	100.00 ± 11.02	98.00 ± 10.13	97.75 ± 12.42	87.00 ± 0.00	0.40
Rat	110.40 ± 11.04	107.80 ± 10.16	106.20 ± 9.04	105.00 ± 9.56	109.00 ± 9.00	101.00 ± 0.00	0.63

Abbreviations: *ONH* optic nerve head, *RT* retinal thickness, *V* vascular area of rabbit retina, *AV* avascular area of rabbit retina. The mean RT for each animal model at increasing distances from the ONH are provided. *P* values comparing RT at all distances within each animal model are shown in the right column. Asterisks indicate significant differences in RT at varying distances from the ONH for that particular animal model.

Table 20.2 Comparison of mean RT between each of the five animal models with increasing eccentricity from the ONH

Distance from ONH (mm)	1	2	3	4	5	6
Total RT	<0.001	<0.001	<0.001	<0.001	<0.001	<0.001
Inner RT	<0.001	<0.001	<0.001	<0.001	<0.001	<0.001
Outer RT	0.029	0.011	0.003	0.001	0.025	<0.001
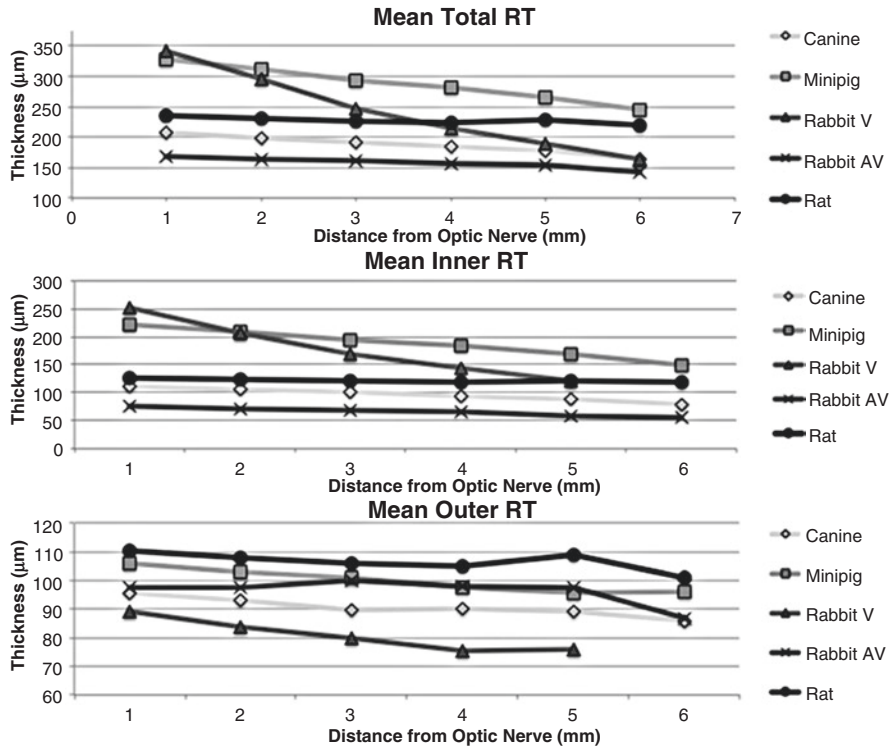
Fig. 20.3 Correlation of the mean RT with increasing eccentricity from the ONH for each animal model

In the rat animal model (Fig. 20.2l–n), there was no statistically significant change in RT with increasing distance from ONH. The mean total RT decreased from 236 to 220 μm ($p = 0.725$); the mean inner RT decreased from 125 to 119 μm ($p = 0.771$); and the mean outer RT decreased from 110 to 101 μm ($p = 0.630$).

Among all animal models, there were statistically significant differences in total RT at similar distances from the ONH ($p < 0.001$; Table 20.2). The same held true for all inner RT and outer RT measurements among the animal models ($p < 0.001$ and $p < 0.029$, respectively; Fig. 20.3).

20.4 Discussion

We demonstrate a standardized approach to reporting retinal thickness measurements in multiple commonly used animal models using SD-OCT. Specifically we quantify the total, inner, and outer RT of healthy canine, mini-pig, rabbit, and rat retina at specific distances from the ONH. In general, total RT and inner RT decreased with increasing distance from the optic nerve head in all the animal models, although with differing magnitudes. The outer RT did not have a similar pattern, and we only detected a change in outer retinal thickness with distance from the ONH in the canine. The greater magnitude and consistency of decrease in inner RT measurements compared to outer RT measurements with increasing distance from the ONH may be attributed to the retinal nerve fiber layer (RNFL).

Among the animal models, there were significant differences in RT at similar distances from the ONH for total, inner, and outer RT. This shows that the healthy canine, mini-pig, rabbit, and rat models each serve as a unique models with significant differences in retinal anatomy. Thus, it is important to establish normative RT for each of these models as in this study, so that they may be used in future studies involving any of the same animals.

Non-OCT-based measurements of normative RT have previously been reported in canine (Hernandez-Merino et al. 2011; Rosolen et al. 2012; Gilger 2014), mini-pig (Rosolen et al. 2012; Gilger 2014), mouse/rat (Remtulla and Hallett 1985; Kim et al. 2008; Nagata et al. 2009; Ferguson et al. 2013; Ruggeri et al. 2007; Gilger 2014; Srinivasan et al. 2006), and rabbit models (Alkin et al. 2013; Ducros et al. 1999; Gilger 2014). These studies are not OCT based but produced results similar to those obtained in this study at equivalent distances from the ONH. Therefore, the validity of SD-OCT-based measurements for in vivo assessment of retinal thickness is demonstrated in this study. Our study also investigates these retinal thickness measurements at 6 points from the ONH (approximately 1 mm apart), offering a more standardized and reproducible approach to measuring RT in various parts of the retina. In addition, we measure specific sections of the cross-sectional retina to include the inner and outer segments, not just the total RT. In this manner, we account for inherent anatomical variations such as the presence of the RNFL in the inner retinal segment.

This study is limited by the reliance on manual measurements of retinal thicknesses, which are subjectively biased. This error was minimized, but not alleviated, with strict criteria for layer boundaries, as defined in our measurement protocol. We also observed that the rabbit vascular streak had lower image quality in the deeper retinal sections compared to the other animal models. This may be attributed to the effect of the thicker RNFL. However, all SD-OCT images obtained were of sufficient quality to measure all layers of interest, with results showing similar findings to histology from previous studies (Alkin et al. 2013).

In most research practice, establishing histological measurements of normal RT provides the main methodology by which to distinguish between diseased and normal animal retinas. However, this method is invasive and time-consuming, making

it difficult to conduct a longitudinal study. SD-OCT is a useful imaging modality that is commonly used in studies involving animal models given its ability to quickly and noninvasively obtain high-resolution, cross-sectional images of the retina. This could reduce the number of animals needed for future quantitative and descriptive studies of the retina while offering more reliable and accurate analysis of the retina over a longer follow-up period.

References

Alkin Z, Kashani AH, Lopez-Jaime GR, Ruiz Garcia H, Humayun MS, Sadda SR (2013) Quantitative analysis of retinal structures using spectral domain optical coherence tomography in normal rabbits. Curr Eye Res 38(2):299–304. https://doi.org/10.3109/02713683.2012.757625. PubMed PMID: 23373715

Costa RA, Skaf M, Melo LA Jr, Calucci D, Cardillo JA, Castro JC et al (2006) Retinal assessment using optical coherence tomography. Prog Retin Eye Res 25(3):325–353. https://doi.org/10.1016/j.preteyeres.2006.03.001. PubMed PMID: 16716639

Drexler W, Fujimoto JG (2008) State-of-the-art retinal optical coherence tomography. Prog Retin Eye Res 27(1):45–88. https://doi.org/10.1016/j.preteyeres.2007.07.005. PubMed PMID: 18036865

Ducros MG, Huang H, Chao LC, Chen Z, Nelson JS, Rylander HG et al (1999) Polarization sensitive optical tomography of the rabbit eye. IEEE J Sel Top Quantum Electron 5(4):1159–1167

Ferguson LR, Dominguez JM, Balaiya S, Grover S, Chalam KV (2013) Retinal thickness normative data in wild-type mice using customized miniature SD-OCT. PLoS One 8(6):e67265. https://doi.org/10.1371/journal.pone.0067265. PubMed PMID: 23826252; PubMed Central PMCID: PMCPMC3695045

Ferguson LR, Grover S, Dominguez JM 2nd, Balaiya S, Chalam KV (2014) Retinal thickness measurement obtained with spectral domain optical coherence tomography assisted optical biopsy accurately correlates with ex vivo histology. PLoS One 9(10):e111203. https://doi.org/10.1371/journal.pone.0111203. PubMed PMID: 25360629; PubMed Central PMCID: PMCPMC4216007

Garcia Garrido M, Beck SC, Muhlfriedel R, Julien S, Schraermeyer U, Seeliger MW (2014) Towards a quantitative OCT image analysis. PLoS One 9(6):e100080. https://doi.org/10.1371/journal.pone.0100080. PubMed PMID: 24927180; PubMed Central PMCID: PMCPMC4057353

Gilger BC (2014) Ocular pharmacology and toxicology. Humana Press/Springer, New York. x, 323 p

Hernandez-Merino E, Kecova H, Jacobson SJ, Hamouche KN, Nzokwe RN, Grozdanic SD (2011) Spectral domain optical coherence tomography (SD-OCT) assessment of the healthy female canine retina and optic nerve. Vet Ophthalmol 14(6):400–405. https://doi.org/10.1111/j.1463-5224.2011.00887.x. PubMed PMID: 22050777

Kim KH, Puoris'haag M, Maguluri GN, Umino Y, Cusato K, Barlow RB et al (2008) Monitoring mouse retinal degeneration with high-resolution spectral-domain optical coherence tomography. J Vis 8(1):17.1–1711. https://doi.org/10.1167/8.1.17. PubMed PMID: 18318620

Nagata A, Higashide T, Ohkubo S, Takeda H, Sugiyama K (2009) In vivo quantitative evaluation of the rat retinal nerve fiber layer with optical coherence tomography. Invest Ophthalmol Vis Sci 50(6):2809–2815. https://doi.org/10.1167/iovs.08-2764. PubMed PMID: 19182247

Remtulla S, Hallett PE (1985) A schematic eye for the mouse, and comparisons with the rat. Vis Res 25(1):21–31. PubMed PMID: 3984214

Rosolen SG, Riviere ML, Lavillegrand S, Gautier B, Picaud S, LeGargasson JF (2012) Use of a combined slit-lamp SD-OCT to obtain anterior and posterior segment images in selected

animal species. Vet Ophthalmol 15(Suppl 2):105–115. https://doi.org/10.1111/j.1463-5224.2012.01037.x. PubMed PMID: 22616780

Ruggeri M, Wehbe H, Jiao S, Gregori G, Jockovich ME, Hackam A et al (2007) In vivo three-dimensional high-resolution imaging of rodent retina with spectral-domain optical coherence tomography. Invest Ophthalmol Vis Sci 48(4):1808–1814. https://doi.org/10.1167/iovs.06-0815. PubMed PMID: 17389515

Sadda SR, Joeres S, Wu Z, Updike P, Romano P, Collins AT et al (2007) Error correction and quantitative subanalysis of optical coherence tomography data using computer-assisted grading. Invest Ophthalmol Vis Sci 48(2):839–848. https://doi.org/10.1167/iovs.06-0554. PubMed PMID: 17251486

Srinivasan VJ, Ko TH, Wojtkowski M, Carvalho M, Clermont A, Bursell SE et al (2006) Noninvasive volumetric imaging and morphometry of the rodent retina with high-speed, ultrahigh-resolution optical coherence tomography. Invest Ophthalmol Vis Sci 47(12):5522–5528. https://doi.org/10.1167/iovs.06-0195. PubMed PMID: 17122144; PubMed Central PMCID: PMCPMC1941766